



ANALYSIS OF ERRORS OF PIEZOELECTRIC SENSORS USED IN WEAPON STABILIZERS

Igor Korobiichuk

Industrial Research Institute for Automation and Measurements PIAP, Al. Jerozolimskie 202, 02-486 Warsaw, Poland
(✉ ikorobiichuk@piap.pl, +48 516 593 540)

Abstract

Effectiveness of operation of a weapon stabilization system is largely dependent on the choice of a sensor, *i.e.* an accelerometer. The paper identifies and examines fundamental errors of piezoelectric accelerometers and offers measures for their reduction. Errors of a weapon stabilizer piezoelectric sensor have been calculated. The instrumental measurement error does not exceed $0.1 \times 10^{-5} \text{ m/s}^2$. The errors caused by the method of attachment to the base, different noise sources and zero point drift can be mitigated by the design features of piezoelectric sensors used in weapon stabilizers.

Keywords: acceleration, piezoelectric sensor, errors, weapon stabilizer.

© 2017 Polish Academy of Sciences. All rights reserved

1. Introduction

Today, there are several types of sensors for *Weapon Stabilization System* (WSS). Each of them has its advantages and disadvantages. Leading technical universities in Ukraine, Poland, USA, Japan, Germany, Russia and other world's leading countries develop new models of WSS accelerometers and increase their accuracy. The paper presents basic types of accelerometers.

As shown by the analysis of WSS accelerometers, the achievable accuracy of aviation accelerometric measurements is currently $(2-10) \times 10^{-5} \text{ m/s}^2$ [1–3]. However, in order to satisfy tasks performed by vehicle weapon stabilizers, accelerometry requires a substantially improved accuracy and speed of measurements. It stems primarily from the necessity for improving the accuracy of accelerometers, developing methods for automatic compensation of acceleration measurement errors, improving the mathematical model of WSS, and solving the problem of filtration of perturbations in the WSS accelerometer output signal [4, 5].

The accuracy of a modern WSS is mainly limited by the accuracy of its accelerometer [6].

Ultimately, we can conclude that attaining a WSS accelerometer accuracy of $1 \times 10^{-5} \text{ m/s}^2$ is currently crucial for a substantial improvement of accuracy of modern WSSs.

Well-known WSS sensors are characterized by the above mentioned advantages but also by their significant disadvantages (Table. 1), which mainly include:

- 1) a low measurement accuracy ($(2-10) \times 10^{-5} \text{ m/s}^2$);
- 2) the necessity for applying a filtering procedure to the WSS sensor output signal;
- 3) instability of the static gear ratio of WSS accelerometers caused by changes in the properties of their structural elements;
- 4) a low speed and inability of in-line data processing, and others.

These disadvantages may be overcome, if a piezoelectric sensor is used as a WSS accelerometer [6]. The research in this field is reasonable, since piezoelectric sensors are

currently the best sensors to use in inertial navigation systems and ballistic missile control systems. These devices have been constructed for use in complex dynamic conditions (an axis acceleration of over 50 g; a temperature range: $-80 \dots +200^{\circ}\text{C}$; an air pressure in an unpressurized box: 700...800 mm Hg at the surface of the Earth and 10^{-6} mm Hg at an altitude of 200 km). Dynamic conditions are less strict when using a *piezoelectric sensor* (PS) as an element of WSS in vehicles [6]. That is why the authors decided to perform more thorough research focusing on the advisability of using piezoelectric accelerometers in WSSs.

Table 1. Comparative analysis of existing WSS accelerometers.

Type	Denotation	Function	Acceleration measurement accuracy, m/s^2	Sensitivity threshold, $\times 10^{-5} \text{ m/s}^2$	Disadvantages
1	2	3	4	5	6
Quartz	GAL	Compensation of acceleration torque by torsion of elastic thread that carries horizontal pendulum	8×10^{-5}	0.3	Big time constant; Insufficient speed; Low accuracy; Low sensitivity
	GI 1/1		6×10^{-5}	0.1	
	Chekan-AM		6×10^{-5}	0.1	
	GRIN-2000/M		5×10^{-5}	0.2	
Spring	GSS	Compensation of torque by vertical spring	10×10^{-5}	0.2	Hard-to-predict drift of elastic properties of string element; Low accuracy
	L-R-S			0.1	
Magnetic	Bell BGM-2, Bell VM-IX, Autonetics VM-7G, MAG-1M, GT-1A, GT-2A	Compensation of acceleration torque by magnetic or electromagnetic spring	8×10^{-5}	0.2	Instability of magnetic properties of permanent magnet; Insufficient speed; Low accuracy
String	GSD-M	Change of string vibration frequency is directly proportional to change of acceleration	8×10^{-5}	0.1	Instability of elastic properties of string; Possibility of resonance; Insufficient speed and accuracy
	GRAVITON-M		5×10^{-5}	0.1	
Gyroscopic	PIGA 16, 25	Turn of platform at an angle sufficient to create a gyroscopic torque that balances pendulosity along input axis of a device	3×10^{-5}	0.1	High net costs; Structural complexity; Insufficient speed and accuracy
	Gyro accelerometer		2×10^{-5}	0.1	

The literature sources [7–12] neither analyze the basic errors, nor study the main characteristics of new PSs [6]. Therefore, the aim of this section is to provide an analysis and necessary study.

The task is to analyze the methodological WSS errors, determine the composition and structure of PS errors, identify the major errors of a new PS and suggest ways to reduce them.

Available vehicle WSSs, which apply quartz, magnetic, spring, string and gyroscopic accelerometers can provide an acceleration measurement accuracy within $(2-10) \times 10^{-5} \text{ m/s}^2$. However, an accuracy of WSS accelerometers is required to be $1 \times 10^{-5} \text{ m/s}^2$ for effective practical application of WSS [6].

The summarized shortcomings of the existing accelerometers for WSSs are eliminated completely or partially due to the use of a piezoelectric element as the WSS accelerometer. WSS contains a piezoelectric element, sensors for determining the object's speed and location coordinates, and current height sensors. Their outputs are connected to a mobile microcontroller

of objects. The piezoelectric accelerometer is located on a double-axis platform, stabilizing its sensitivity axis vertically. The sensor of the WSS piezoelectric sensing element consists of a piezoelectric element, working on the compression-stretching strain, with insulators on its both ends and inertial mass. The piezoelectric element is a multi-layer structure (piezo-pack) consisting of crystal lithium niobate layers with antiparallel polarization and electrodes separated by connecting layers.

2. Piezoelectric sensor errors

To analyze the PS errors, the following classification should be introduced: by the error factors (the methodical factor, caused by an imperfect measurement method or a mismatched model, and the instrumental factor, caused by measuring device properties), by their effects (static and dynamic); by their repeatability (the random errors, varying randomly in sign and value during repeated measurements of the same value, and the systematic errors, remaining during the same measurements either constant or varying according to expectations) [13, 3].

2.1. Instrumental errors

The instrumental PS error is determined as the sum of errors of all values that directly affect the final output of accelerometer [13].

The basic working formula of converting acceleration to voltage is as follows:

$$U_{out} = \frac{d_{ij} \cdot m \cdot g_z}{C_{PS}}, \quad (1)$$

where: U_{out} is the output PS voltage; g_z is the *gravitational acceleration* (GA); d_{ij} is the piezoelectric modulus; m is the mass of PS and IM; C_{PS} is the electric capacity of PS.

The true value of GA is determined by the formula:

$$g_z = \frac{U_{out} \cdot C_{PS}}{d_{ij} \cdot m}. \quad (2)$$

The relative error of output signal equals to the sum of multiplications of relative parameter errors by parameter exponents:

$$\frac{\Delta g_z}{g_z} = \frac{\Delta U_{out}}{U_{out}} + \frac{\Delta C_{PS}}{C_{PS}} - \frac{\Delta d_{ij}}{d_{ij}} - \frac{\Delta m}{m}. \quad (3)$$

Let us consider each component of an error:

- 1) To calculate the piezoelectric modulus variation error, it is worth mentioning that the new PS is made of lithium niobate. At a temperature variation the piezoelectric modulus changes according to the law:

$$\Delta d_{ij} = d_{ij} \alpha_{ic} \Delta t, \quad (4)$$

where α_{ic} is the temperature coefficient of linear expansion of quartz, Δt is the temperature variation value.

The temperature variation error of the piezoelectric modulus:

$$\left(\frac{\Delta d_{ij}}{d_{ij}} \right) = \alpha_{ic} \Delta t. \quad (5)$$

For lithium niobate $\alpha = 0.59 \cdot 10^{-6} \text{C}^{-1}$ [14, 15], then:

$$\left(\frac{\Delta d_{ij}}{d_{ij}} \right) = 0.59 \cdot 10^{-6} \cdot 1 = 0.59 \cdot 10^{-6}. \quad (6)$$

2) To calculate the electrical capacitance variation error, we should use the formula:

$$C_{PS} = \frac{\varepsilon \cdot S}{d}, \quad (7)$$

where: ε is the lithium niobate dielectric constant; S is the PS area; d is the PS height.

As can be seen from (7), the electrical capacitance error depends on the dielectric constant variation and the area affected by the gravitational acceleration. In accordance with the characteristics of dependence of lithium niobate dielectric constant variation on temperature variation, ε varies by 0.5% for the temperature change from 0°C to +500°C. For 1°C it is 0.001%. Consequently, the dielectric constant variation error is:

$$\left(\frac{\Delta\varepsilon}{\varepsilon} \right) = 1 \cdot 10^{-5}. \quad (8)$$

The relative PS area variation error $\frac{\Delta S}{S}$:

$$\frac{\Delta S}{S} = \frac{\Delta b}{b} + \frac{\Delta l}{l}, \quad (9)$$

where: $b = 20 \cdot 10^{-3}$ m and $l = 25 \cdot 10^{-3}$ m are the width and length of PS; respectively; Δl , $\Delta b = 0.8$ mkm are the tolerances for PS area sides.

Then:

$$\frac{\Delta S}{S} = \frac{0.8 \cdot 10^{-6}}{20 \cdot 10^{-3}} + \frac{0.8 \cdot 10^{-6}}{25 \cdot 10^{-3}} = 0.72 \cdot 10^{-4}. \quad (10)$$

The PS height variation error $\frac{\Delta d}{d}$, when $\Delta d = 0.3$ mkm, is:

$$\frac{\Delta d}{d} = \frac{0.3 \cdot 10^{-6}}{5 \cdot 10^{-3}} = 0.6 \cdot 10^{-4}. \quad (11)$$

Thus, the electrical capacitance variation error is equal to:

$$\frac{\Delta C_{PS}}{C_{PS}} = \frac{\Delta\varepsilon}{\varepsilon} + \frac{\Delta S}{S} - \frac{\Delta d}{d} = 0.1 \cdot 10^{-4} + 0.72 \cdot 10^{-4} - 0.6 \cdot 10^{-4} = 0.22 \cdot 10^{-4}. \quad (12)$$

3) To calculate the sensor mass variation error, we should use the formula:

$$m = \rho \cdot V, \quad (13)$$

where: ρ is the lithium niobate density; V is the PS volume; d is the PS height.

The PS density variation error mainly depends on the ambient temperature, so, by an analogy to the piezoelectric modulus variation error, we obtain:

$$\left(\frac{\Delta\rho}{\rho} \right) = \alpha_{tc} \Delta t, \quad (14)$$

where $\alpha_{tc} = 0.59 \cdot 10^{-6} \text{C}^{-1}$ [14, 15] is the temperature coefficient of linear expansion of quartz, Δt is the temperature variation value.

The relative PS density variation error:

$$\left(\frac{\Delta\rho}{\rho} \right) = 0.59 \cdot 10^{-6} \cdot 1 = 0.59 \cdot 10^{-6}. \quad (15)$$

The PS volume variation error is calculated as follows:

$$\left(\frac{\Delta V}{V} \right) = \frac{\Delta S}{S} + \frac{\Delta d}{d} = 0.72 \cdot 10^{-4} + 0.6 \cdot 10^{-4} = 1.32 \cdot 10^{-4}. \quad (16)$$

Thus, the PS mass variation error is equal to:

$$\frac{\Delta m}{m} = \frac{\Delta \rho}{\rho} + \frac{\Delta S}{S} + \frac{\Delta d}{d} = 0.59 \cdot 10^{-6} + 0.72 \cdot 10^{-4} + 0.6 \cdot 10^{-4} = 1.32 \cdot 10^{-4}. \quad (17)$$

- 4) The voltage variation error is determined according to the following consideration. Since the maximum PS instrumental error does not exceed 0.1 mGal (much lesser than the PS cumulative error of 1 mGal), *i.e.* $1 \cdot 10^{-5} \text{ m/s}^2$, we obtain:

$$\frac{\Delta U_{out}}{U_{out}} = \frac{\Delta g_z}{g_z} - \frac{\Delta C_{PS}}{C_{PS}} + \frac{\Delta d_{ij}}{d_{ij}} + \frac{\Delta m}{m} = 0.01 \cdot 10^{-4} - 0.22 \cdot 10^{-4} + 0.0059 \cdot 10^{-4} + 1.3 \cdot 10^{-4} = 1.1 \cdot 10^{-4}. \quad (18)$$

The error values are summarized in Table 2.

Table 2. The PS instrumental errors.

No	Components of instrumental error value	Error value
1	Voltage variation, $\frac{\Delta U}{U}$	$1.1 \cdot 10^{-4}$
2	Piezoelectric variation, $\frac{\Delta d_{ij}}{d_{ij}}$	$0.0059 \cdot 10^{-4}$
3	PS electrical capacitance variation, $\frac{\Delta C_{PS}}{C_{PS}}$	$0.22 \cdot 10^{-4}$
4	Mass variation, $\frac{\Delta m}{m}$	$1.3 \cdot 10^{-4}$
Cumulative instrumental error		$1 \cdot 10^{-6}$

2.2. Error due to mechanical mounting of piezoelectric accelerometer to base

Special attention shall be given to the way of mounting PS to the *horizontally stabilized platform* (HSP) or another base. It is typically an elastic coupling (Fig. 1).

Deficiencies in mounting PS to the base (wrong way of mounting) can lead to significant PS errors.

The errors mainly affect the PS frequency response (appearance of resonances). Errors of this type are insignificant at frequencies up to 200 Hz, Otherwise, they significantly affect PS values. There is a diagram of dependence of mounting methods on the base oscillation frequency values (Fig. 2).

There is a general requirement valid for each mounting method: an almost ideal condition of the base surface.

Screwed pins (3 pieces) should be chosen from the diagram in Fig. 2 as the mounting method. This mounting method corresponds to quite a large working range of PS. That is, the error occurs only at measurement frequencies greater than 10 kHz.

Small parts at the polished base surface should be avoided.

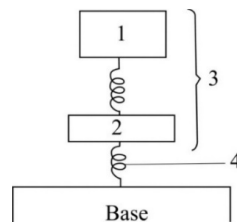


Fig. 1. A mechanical model of PS: 1 – SE; 2 – PS base; 3 – PS; 4 – the mounting method.

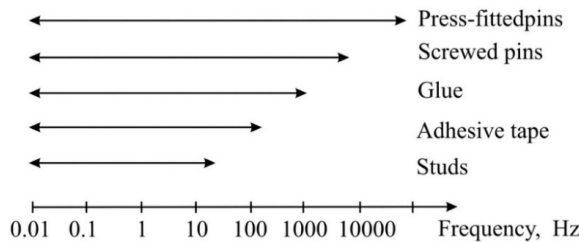


Fig. 2. The dependence of used mounting methods on the operating range of base oscillation frequencies.

2.3. Error caused by different noise sources

There are different types of noise in measurement systems. They are caused by various factors. Therefore, to ensure accurate PS indications, each possible noise should be taken into account and PS should be designed so as to reduce noise to a level at which either it can be neglected in the first approximation, or its impact eliminated.

One of the main types of noise to be primarily reduced is the noise caused by capacitive coupling in PS structure.

The most common way to reduce or eliminate the impact of such noise is to connect the sensor with the measurement circuit by a shielded or coaxial cable. However, this method of avoiding noise involves a relatively small length of shielded cables. Also, the coaxial cable is exposed to moisture which eventually results in decreasing its performance.

The most effective way to deal with the capacitive noise is to use a twisted pair wire, known as the equilibrium (twisted) pair. Since mutual interference in each point of twisted pair results in contraflow, the effect from its action is almost zero at the amplifier input.

After selecting a type of cable, it is necessary to consider the impact of noise on PS figures caused by connecting this cable with the PS construction. Indeed, distortion or displacement of insulation relative to conductors generates a charge motion, mainly under the piezoelectric effects and due to a change of spatial capacity allocation. Such noise can be reduced, if the cable is tightly fixed to the vibrating construction of the perturbed section.

One of circuit designs, enabling a reduction of interference caused by noise, is the use of a protective ring. The high-resistance amplifier input is connected to a low-resistance protection, which is equipotential with respect to the input. Such an amplifier is non-inverting (serves as a buffer). Therefore, its output signal is equal to the input signal, and its output resistance is much less than the input one. The protective ring is directly connected with the amplifier output and forms a low-resistance input to signals from any parasitic coupling.

The acoustic noise also have an impact on PS figures. In particular, this impact is significant during measuring GA. Such noise directly affects PS and place of its mounting to the construction. The level of errors can be illustrated by the fact that the parasitic signal of PS may be about 0.001 g at a sound pressure level of 100 dB.

However, a new PS and a body-base system are well isolated from each other, and it provides a significant resistance to the acoustic noise.

2.4. Error caused by piezo-element zero-point shift

One of disadvantages of accelerometers, which is almost impossible to eliminate, is the zero-point shift or drift. The zero-point shift is reflected in the fact that the PS index always slowly shifts at the same place and in constant conditions (temperature and pressure). So, the readings taken today are different from those taken yesterday. The shift depends on several factors: the ambient temperature, the signal mode and others. The nature of this shift is that the strained

elastic element of accelerometer (spring, twisted thread or, as in our case, piezo-element) does not precisely follow the law of proportional strain. There is a “fatigue” of the elastic element due to tension, so it is gradually changing its deformation at a constant load [17].

The zero-point shift varies in different systems and for different materials from tenths of mGal to several mGal per day.

The error in a new PS caused by the zero-point shift can be equal to zero for a long time. This is because at low and average temperatures it remains stable, and a feedback loop included in the system constantly returns PS to its original position, compensating for the input load.

2.5. Error caused by atmospheric pressure change

The atmospheric pressure can reduce, to some extent, the load on PS, *i.e.* it is affected only by G' , rather than by the whole strength of gravity $G = m \cdot g_z$ [8]:

$$G' = m g_z \left(1 - \frac{\rho_a}{\rho_m}\right), \quad (19)$$

where: ρ_a is the air density; ρ_m is the sensor's material density.

As the material of a new PS is lithium niobate, its density is $\rho_m = 4640 \text{ kg/m}^3$, and the air density is $\rho_a = 1.2 \text{ kg/m}^3$ at a normal atmospheric pressure (101 325 Pa) and temperature 200°C [14, 15]. Substituting these data into the formula (19), we obtain:

$$G' = m g_z \left(1 - \frac{1.2}{4640}\right) = (1 - 0.00026) \cdot m g_z. \quad (20)$$

As we see from the formula (20), the gravity decreases by 26 mGal at the required accuracy of 1 mGal (10^{-5} m/s^2). This error is calculated for PS working conditions at low altitudes. However, an increase in height entails a decrease in the atmospheric pressure averagely by 11 mm Hg per 100 m and in the ambient temperature by 6°C per 1 km, which causes a change in density of both air and lithium niobate. This phenomenon makes the error unpredictable and difficult for software to calculate and compensate.

There are two ways to ensure stability of PS system to changes in the atmospheric pressure, the first of which is to apply a barometric compensation. This method involves placing PS in a special vacuum chamber that maintains a constant atmospheric pressure. However, it does not protect PS from the adiabatic temperature effect, causing significant errors at a high altitude, and significantly increases its overall size.

Another way to eliminate the impact of atmospheric pressure changes, which is optimal for the PS design as an element of WSS, is pressurizing the PS. That is, the PS and measuring circuit are placed in a sealed enclosure made of a material resistant to changes in the atmospheric pressure and air. PS pressurizing eliminates an influence of error caused by changes in the atmospheric pressure.

2.6. Errors of transient (relative to device) angular velocity

Errors of the transient (relative to the device) angular velocity ω_z are determined by the formula [3]:

$$\Delta_E = K_{PG} \omega_E, \quad (21)$$

$$\delta_E = \frac{\Delta_E}{\alpha_{us}} \cdot 100\%, \quad (22)$$

where: K_{PG} is the PS transfer coefficient; ω_E is the Earth rotational rate; α_{us} is the PS useful signal.

We find the analytical error expression Δ_E , considering that the vertical component of transient angular velocity of the main axis $xOyz$ is caused by the Earth's rotation and motion of a vehicle:

$$\omega_z = \omega_E \sin \phi + \frac{V_s}{r} \operatorname{tg} \phi, \quad (23)$$

$$v_s = r \dot{\lambda} \cos \phi, \quad (24)$$

$$\frac{V_s}{r} \operatorname{tg} \phi = \dot{\lambda} \sin \phi, \quad (25)$$

where v_s is the easterly component of vehicle ground speed; r is the geocentric radius of the Earth; $\dot{\lambda}$ is the longitudinal change rate.

Given (25), the expression (23) can be presented as:

$$\omega_z = (\omega_E + \dot{\lambda}) \sin \phi. \quad (26)$$

In general, a vehicle is rotated around the axis Oz at the angular velocity \dot{k} and we have:

$$\omega_z = (\omega_E + \dot{\lambda}) \sin \phi + \dot{k}, \quad (27)$$

where k is the horizontal course angle, measured clockwise from the north to the longitudinal axis of the object.

Given (27), the expression (21) can be written as:

$$\Delta_E = K_{PG} [(\omega_E + \dot{\lambda}) \sin \phi + \dot{k}]. \quad (28)$$

The corresponding average value of the absolute error $\overline{\Delta_E}$ is:

$$(t_2 - t_1) \overline{\Delta_E} = K_{PG} [k(t_2) - k(t_1)] + K_{PG} \int_{t_1}^{t_2} \omega_E \sin \phi(t) dt + K_{PG} \int_{t_1}^{t_2} \dot{\lambda}(t) \sin \phi(t) dt, \quad (29)$$

where $(t_2 - t_1)$ is the averaging interval.

The maximum value of the term $K_{PG} \omega_E \sin \phi$, corresponding to $\phi = 90^\circ$, and the Earth rotational rate $\omega_E = 7.29 \cdot 10^{-5} \text{ s}^{-1}$, is $2.92 \cdot 10^{-5} \text{ rad}$ [18].

Apparently, the calculation error of the term at stable ω_E and specified k depends on the calculation error of ϕ . Assuming that the calculation error of $K_{PG} \omega_E \sin \phi$ should not exceed $0.01\% = 2.92 \cdot 10^{-7} \text{ rad}$, we can easily calculate that the latitude calculation error should not exceed 0.5° .

Note: the latitude calculation error is less than 0.5° , if for the averaging interval $(t_2 - t_1)$ the average value $\overline{\sin \phi}$ is substituted for $\int_{t_1}^{t_2} \sin \phi(t) dt$. Besides, since the flights are performed with a constant velocity, the average value $\overline{\phi}$ corresponds to the midpoint of $(t_2 - t_1)$, and $\overline{\sin \phi}$ differs from $\sin \overline{\phi}$ insignificantly, so:

$$K_{PG} \int_{t_1}^{t_2} \omega_E \sin \phi(t) dt = K_{PG} \omega_E \sin \overline{\phi} (t_2 - t_1). \quad (30)$$

WSS sensitivity to the latitude calculation error is maximal at the mid latitude motion of a vehicle. So let us define the term $\dot{\lambda}(t) \sin \phi$ at $\phi = 65^\circ$ and $v_y = 234 \text{ m/s}$, $r = 6.4 \cdot 10^6 \text{ m}$:

$$\dot{\lambda}(t) \sin \phi = 7.3 \cdot 10^{-5} \text{ c}^{-1}. \quad (31)$$

Consequently, at the predetermined parameters of motion $\dot{\lambda}(t)\sin\varphi$ is equal to the angular velocity of the Earth.

If $\dot{\lambda}(t)$ integral is taken for short time intervals that can be considered constant, we can use the equation:

$$K_{PG} \int_{t_1}^{t_2} \dot{\lambda}(t) \sin \phi(t) dt = K_{PG} [\lambda(t_2) - \lambda(t_1)] \sin \bar{\varphi}, \quad (32)$$

where φ is adjusted as an averaging interval midpoint.

During the test program, a route should be chosen along a parallel (in this case a latitude is almost constant, so the predetermined φ can be used in calculations) or a meridian (in this case, a series expansion can be used for relatively crude approximation of $\sin \bar{\varphi}$). When consolidating the flight data for calculating $\bar{\varphi}$, the interval midpoint ($t_2 - t_1$) should be used.

We write the expression (24) in its final form:

$$\Delta_E = K_{PG} \left(\frac{k(t_2) - k(t_1)}{t_2 - t_1} + \omega_E \sin \bar{\varphi} + \frac{\lambda(t_2) - \lambda(t_1)}{t_2 - t_1} \sin \bar{\varphi} \right). \quad (33)$$

Let us calculate $\bar{\Delta}_E$ and $\bar{\delta}_E$ for the above parameters, when $\dot{k} = 0$. In this case $\bar{\Delta}_E = 5.8 \cdot 10^{-5}$ rad = 584×10^{-5} m/s² and $\bar{\delta}_E = 2.92 \cdot 10^{-2}\%$.

Therefore, the PS error caused by ω_z is large compared to other errors. It should be considered when introducing amendments in the equation of WSS motion.

The expression (33) shows that in order to reduce the error of transient angular velocity around the PS axis, we should reduce the transmission factor of instrumentation channel by changing the PS design.

3. Conclusions

The research enables to solve a relevant and complex scientific and technical task that is paper identifies and examines the fundamental errors of piezoelectric accelerometers.

Reduction of each type of error is suggested by certain measures (the instrumental error is 0.1×10^{-5} m/s²).

The composition and structure of PS errors are defined. The main of them are considered and calculated. The instrumental error does not exceed 0.1×10^{-5} m/s². The errors caused by the way of attachment to the base, different noise sources and zero point drift can be eliminated by the design features of PS.

Acknowledgements

This work was supported by the Ministry of Education and Science of Ukraine (grant № 0115U002089).

References

- [1] Lai, A., James, D.A., Hayes, J.P., Harvey, E.C. (2004). Semi-automatic calibration technique using six inertial frames of reference. *Proc. of SPIE × The International Society for Optical Engineering*, 5274, 531–542.
- [2] Lakehal, A., Ghemari, Z. (2016). Suggestion for a new design of the piezoresistive accelerometer. *Ferroelectrics*, 493(1), 93–102.
- [3] Korobiichuk, I., Bezvesilna, O., Tkachuk, A., Nowicki, M., Szewczyk, R., Shadura, V. (2015). Aviation gravimetric system. *International Journal of Scientific & Engineering Research*, 6(7), 1122–1127.

- [4] Liu, Y., Ji, T., *et al.* (2016). Calibration and compensation for accelerometer based on Kalman filter and a six-position method. *Yadian Yu Shengguang/Piezoelectrics and Acoustooptics*, 38(1), 94–98, 110.
- [5] Gao, J.M., Zhang, K.B., *et al.* (2015). Temperature characteristics and error compensation for quartz flexible accelerometer. *International Journal of Automation and Computing*, 12(5), 540–550.
- [6] Korobiichuk, I. (2016). Mathematical model of precision sensor for an automatic weapons stabilizer system. *Measurement*, <http://dx.doi.org/10.1016/j.measurement.2016.04.017>.
- [7] Korobiichuk, I., Bezvesilna, O., *et al.* (2016). Design of piezoelectric gravimeter for automated aviation gravimetric system. *Journal of Automation, Mobile Robotics & Intelligent Systems (JAMRIS)*, 10(1).
- [8] Korobiichuk, I., Bezvesilna, O., *et al.* (2016). Piezoelectric gravimeter of the aviation gravimetric system. *Advances in Intelligent Systems and Computing* 440. Szewczyk, R., Zieliński, C., Kaliczyńska, M. (eds.), *Challenges in Automation, Robotics and Measurement Techniques. Proc. of AUTOMATION-2016*, Warsaw, Poland, 753–763.
- [9] Korobiichuk, I., Bezvesilna, O., *et al.* (2015). Stabilization system of aviation gravimeter. *International Journal of Scientific & Engineering Research*, 6(8), 956–959.
- [10] Fan, C., Hu, X., *et al.* (2014). Observability analysis of a MEMS INS/GPS integration system with gyroscope G-sensitivity errors. *Sensors*, 14(9), 16003–16016.
- [11] Quinchia, A.G., Falco, G., Falletti, E., Dovis, F., Ferrer, C. (2013). A comparison between different error modeling of MEMS applied to GPS/INS integrated systems. *Sensors*, 13(8), 9549–9588.
- [12] Karachun, V., Mel'nick, V., Korobiichuk, I., Nowicki, M., Szewczyk, R., Kobzar, S. (2016). The Additional Error of Inertial Sensor Induced by Hypersonic Flight Condition. *Sensors*, 16(3).
- [13] Lobanov, V.S., Tarasenko, N.V., *et al.* (2007). Fiber-optic gyros & quartz accelerometers for motion control. *IEEE Aerospace and Electronic Systems Magazine*. 22(4), 23–29.
- [14] Guo, Y., Kakimoto, K.I., Ohsato, H. (2005). (Na_{0.5}K_{0.5})NbO₃-LiTaO₃ lead-free piezoelectric ceramics. *Materials Letters*, 59(2–3), 241–244.
- [15] Tables of fundamental properties of piezoceramic materials manufactured by Ferropiezoelectric Material Division, devices and tools of Research Institute of Physics SFU [electronic resource]. – Access mode, <http://www.piezotech.ru/PKR.htm>.
- [16] Arlou, Y.Y., Tsyantenka, D.A., Sinkevich, E.V. (2015). Wideband computationally-effective worst-case model of twisted pair radiation. *Proc. of the International Conference Days on Diffraction*, 14–19.
- [17] Meggiolaro, M.A., Castro, J.T.P.D., Góes, R.C.D.O. (2016). Elastoplastic nominal stress effects in the estimation of the notch-tip behavior in tension. *Theoretical and Applied Fracture Mechanics*.
- [18] Korobiichuk, I., Koval, A., Nowicki, M., Szewczyk, R. Investigation of the Effect of Gravity Anomalies on the Precession Motion of Single Gyroscope Gravimeter. *Solid State Phenomena*, 251, 139–145.